ELSEVIER

Chemical Engineering Journal 142 (2008) 263–270

Chemical Engineering Journal

www.elsevier.com/locate/cej

Swelling/deswelling kinetics of PNIPAAm hydrogels synthesized by microwave irradiation

Z.X. Zhao, Z. Li *, Q.B. Xia, E. Bajalis, H.X. Xi, Y.S. Lin

School of Chemical and Energy Engineering, South China University of Technology, Guangzhou, Guangdong 510641, China

Received 13 July 2007; received in revised form 14 November 2007; accepted 4 December 2007

Abstract

This work involves the study of swelling and deswelling kinetics of poly(*N*-isopropylacrylamide) (PNIPAAm) hydrogels separately synthesized by means of microwave irradiation and normal water-bath heating. The swelling and deswelling kinetic curves of the PNIPAAm hydrogels were measured in water below and above the lower critical solution temperature (LCST), and their swelling and deswelling kinetic parameters were estimated. Textural properties and surface morphology of these PNIPAAm hydrogels were characterized by accelerated surface area and porosimetry apparatus and SEM. The effects of textural properties on their swelling and deswelling kinetic behavior were discussed. Results showed that swelling and deswelling rates of the synthesized PNIPAAm hydrogels increased with temperature, and the deswelling rates of these hydrogels were higher than their swelling rates. As compared with the PN hydrogel synthesized by the conventional method, the PM hydrogel synthesized by microwave irradiation had larger swelling and deswelling rate constants as well as lower swelling/deswelling activation energy due to its higher surface area and larger pore sizes, and thus it had faster response behavior.

Keywords: PNIPAAm hydrogels; Swelling/deswelling kinetics; Activation energy; Microwave irradiation

1. Introduction

Poly(*N*-isopropylacrylamide), PNIPAAm, has been extensively studied as the best-known thermo-sensitive polymeric network [1]. It exhibits a reversible phase transition induced by a small external temperature change about its lower critical solution temperature (LCST) at around 32 °C in aqueous media [2–4]. PNIPAAm is soluble in water at low temperature, but its phase separates as soon as temperature exceeds its LCST [5]. Along with its phase transition, its physical or chemical properties are changed dramatically, such as network structure, swelling and heterogeneous properties. Because of this unique property, the gel is expected to have applications in the bioengineering and biotechnological fields [6].

However, a drawback of conventional PNIPAAm hydrogels is their slow response behavior because of their dense and thick skin layer formed at the beginning of the phase transition [1]. This would limit its wide application in controlled drug delivery systems, artificial organs and on–off switch [6]. With a fast response rate, the hydrogels can be used to make accurate and sensitive sensor, medicine controlled release carrier and artificial muscles or some such things. Therefore, improvement of response behavior of the PNIPAAm hydrogels and estimation of their response rate are necessary.

Many researchers have investigated some factors affecting the response rate of the thermo-sensitive hydrogels. As shown in many past studies, the porous structure of PNIPAAm hydrogels has a strong impact on their swelling and deswelling rate. Several efforts have been made to improve the response rate for such hydrogels via either the change of chemical and/or physical structures. Zhang et al. [6] used water and tetrahydrofuran as a mixed solvent to modulate the matrix structure of PNIPAAm hydrogel and found that the hydrogels were highly porous and exhibited very rapid swelling and deswelling rate. Eder et al. [7] prepared the PNIPAAm gels by e-beam irradiation. The shrinking kinetics experiments demonstrated that e-beam crosslinked gels responded to temperature changes up to 20 times faster than the chemical crosslinked ones due to its much more porous surface with micron-sized channels formation while swelling. Serizawa et al. [8] prepared porous PNIPAAm by incorporation silica micro-particles and reported that the deswelling rate was at least 80 times greater than that of the conventional

---

* Corresponding author. Fax: +86 20 87110608.
E-mail address: cezhli@scut.edu.cn (Z. Li).

1385-8947/$ – see front matter © 2007 Elsevier B.V. All rights reserved.
doi:10.1016/j.cej.2007.12.009

Nomenclature

A	rate coefficient
A_d	deswelling rate coefficient
A_s	swelling rate coefficient
E	activation energy
E_d	activation energy of the deswelling (kJ/mol)
E_s	activation energy of the swelling (kJ/mol)
K	rate constant
K_d	deswelling rate constant
K_s	swelling rate constant
q_md	amount absorbed water of equilibrium–deswelling hydrogel in the aqueous solution (g/g)
q_ms	amount absorbed water of equilibrium–swelling hydrogel in the aqueous solution (g/g)
q_t	water amount taken by PNIPAAm hydrogel at time t from the aqueous solution (g/g)
q_0	amount absorbed water of fully swollen hydrogels at 14 °C (g/g)
r_d	deswelling rate
r_s	swelling rate
R	mole gas constant, 8.314 J K^{-1} mol^{-1}
t	time (s or min)

hydrogels, when the temperature increased above the LCST of PNIPAAm.

The main objective of this work is to study the response kinetics of the porous PNIPAAm hydrogels synthesized by microwave irradiation. The swelling and deswelling kinetic experiments of the PNIPAAm hydrogels in water were conducted below and above the lower critical solution temperature (LCST), and corresponding swelling and deswelling kinetic curves and kinetic rate coefficients were determined. The swelling and deswelling activation energies of the PNIPAAm hydrogels were estimated according to the Arrhenius equation. The morphological and textural properties of the synthesized PNIPAAm hydrogels were characterized by scanning electron microscope (SEM) and an accelerated surface area and porosimetry apparatus (ASAP 2010). The impact of the morphological and textural properties of the PNIPAAm hydrogels on their response kinetics would be discussed and reported here.

2. Experimental

2.1. Materials

N-Isopropylacrylamide (NIPAAm, 97% pure) as monomer and *N*,*N*′-methylenebisacrylamide (BIS, 99% pure) were supplied from Aldrich, USA and recrystallized by hexane. 2,2′-Azobis(isobutyronitrile) (AIBN, 99%) was purchased from YiNeng Chromatogram. Acetone was obtained from Shantou Chemical Reagent Factory. The last two were analytical grade. Water was deionized before use.

2.2. Instruments

Mars5 microwave accelerator with adjustable and controllable temperature was purchased from CEM. Its frequency is 2450 kHz and the output power ranged from 300 to 1200 W.

The shapes and surface morphology of the PNIPAAm hydrogels were examined on a scanning electron microscope (SEM), H520SEM, OXFORD. Porous structure of the hydrogels was characterized using an automatic physisorption analyzer (ASAP 2010) by BET method through N_2 adsorption at 77 K.

2.3. Hydrogels synthesis

Normal water-bath heating method was described as follows [9,10]: first, the monomer (*N*-isopropylacrylamide, 1.50 g), cross-linker (*N*,*N*′-methylenebisacrylamide, 150 mg), and initiator [azobis(isobutyronitrile), 164 mg] were dissolved in 15 mL of degassed acetone and then injected into a rockered flask. After that, the flask was kept under N_2 atmosphere, and then the degassed acetone solution was evenly allocated to four separate tiny reactors (10 mm × 150 mm diameters). The polymerization took place at 80 °C by hydrothermal method. After 24 h of gelation, the prepared PNIPAAm hydrogel was removed from the tiny reactors and immersed in pure water for 48 h to remove all non-reactive materials. After drying overnight under the vacuum, the PNIPAAm hydrogel synthesized by water-bath heating was denoted as PN.

Microwave irradiation method: first, the reaction mixture with the same weight ratios as the water-bath heating method was dissolved in 15 mL of degassed acetone and bubbled N_2 for 60 min at room temperature. After that, the solution was transferred to the tiny reactors, and then put into a special microwave reactor. The polymerization reaction was then carried out in the Mars5 microwave accelerator at 80 °C. Reaction temperature was measurable and controlled within ±0.05 °C. The maximum power output was set to 300 W. The reaction duration was set to 30 min. After 24 h of gelation, the prepared PNIPAAm hydrogel was removed from the tiny reactors and immersed in pure water for 48 h to remove all non-reactive materials. After drying overnight under the vacuum, the PNIPAAm hydrogel synthesized by microwave irradiation was denoted as PM.

2.4. Experimental methods

2.4.1. Swelling kinetic studies [6]

Swelling kinetic experiments were carried out by immersing a known amount of the dried hydrogels with 100 mL of distilled water in a constant temperature oven at the temperature below its LCST. Gravimetrical measurement method [6] was used to measure the swelling rat of the gels.

At pre-determined time intervals, the hydrogels were drawn from water, and then surface water of the hydrogels were wiped with moistened filter paper completely, after that, the weights of the hydrogels were measured and recorded until they approached constant. Finally, swelling kinetic data/curve can be available. Swelling kinetic experiments were carried out by immersing a known amount of the fully swollen hydrogels in the range between 14 and 27 °C below its LCST.

2.4.2. Deswelling kinetic studies

Deswelling kinetic experiments were carried out by immersing a known amount of the fully swollen hydrogels at 14.0 °C with 100 mL of the distilled water on a constant temperature oven. At pre-determined time intervals, the hydrogels were drawn from water. After that surface water of the hydrogel was wiped with moistened filter paper completely. Finally, the weight of the hydrogel was measured and recorded until they approached constants. This deswelling procedure was done in the range between 33 and 45 °C above its LCST.

3. Results and discussion

3.1. SEM studies

Figs. 1 and 2 show the SEM photographs of dried and swollen PN and PM hydrogels. A comparison of Figs. 1 and 2 can shows the effects of the preparation methods on the network parameters of the hydrogels PN and PM. It can be seen from Figs. 1 and 2 that the surface texture of PM had higher porosity than that of PN in both dried and swollen states, which suggests that the application of microwave irradiation to prepare PNIPAAm gel made the gel more porous in comparison with the application of the water-bath heating method. The PN and PM hydrogels in Fig. 2 clearly exhibited a characteristic three-dimensional coral-like pattern when they were in the swollen state. Smaller pores were confined by the alveolate wall of the polymer matrix. However, the PM gel had more uniform and deeper pores compared to the PN hydrogel, as shown in Fig. 2c and 2d.

Table 1
The parameters of the porous structure of the PN and PM hydrogels

Sample	BET (S_{BET}, m^2/g)	Pore volume (V_{pore}, cm^3/g)	Average pore size (D_{p}, nm)
PN	1.1088	1.532×10^{-3}	2.37
PM	10.264	2.720×10^{-2}	2.91

These SEM photographs can clearly show the difference in the surface network structure of PN and PM. The PM hydrogel exhibited more porous while the PN hydrogel showed higher crosslinking density. It indicates that in comparison with the water-bath heating method, the use of microwave irradiation method to prepare the hydrogel not only made it more porous, but also made its pores more uniform and deeper. Such a difference in network structure of PN and PM as shown in Figs. 1 and 2 would have an influence on their swelling/deswelling behavior.

3.2. Textural properties of the PNIPAAm hydrogels

Aporosimeter system (ASAP 2010, Micromeritics) was used to determine the textural properties of the PNIPAAm hydrogels. Table 1 lists the pore structure properties, including S_{BET}, V_{pore} and D_{p} of the PN and PM hydrogels, respectively, synthesized by microwave irradiation and conventional water-bath heating.

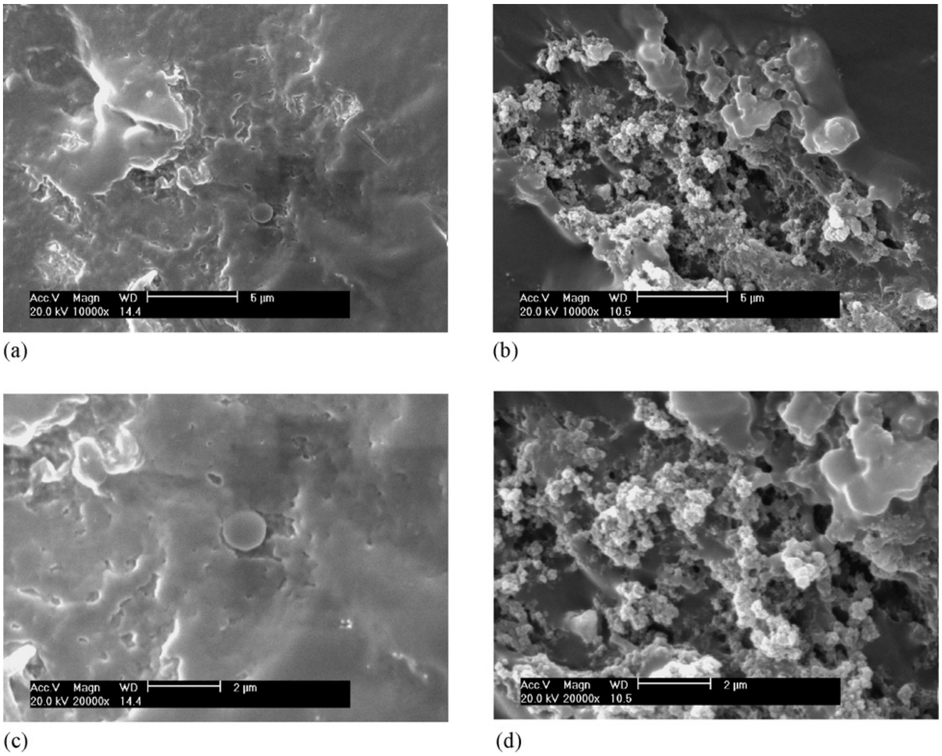

Fig. 1. (a) SEM micrographs of the air-dried PN gel surface (magnification, 10,000×). (b) SEM micrographs of the air-dried PM gel surface (magnification, 10,000×). (c) SEM micrographs of the air-dried PN gel surface (magnification, 20,000×). (d) SEM micrographs of the air-dried PM gel surface (magnification, 20,000×).

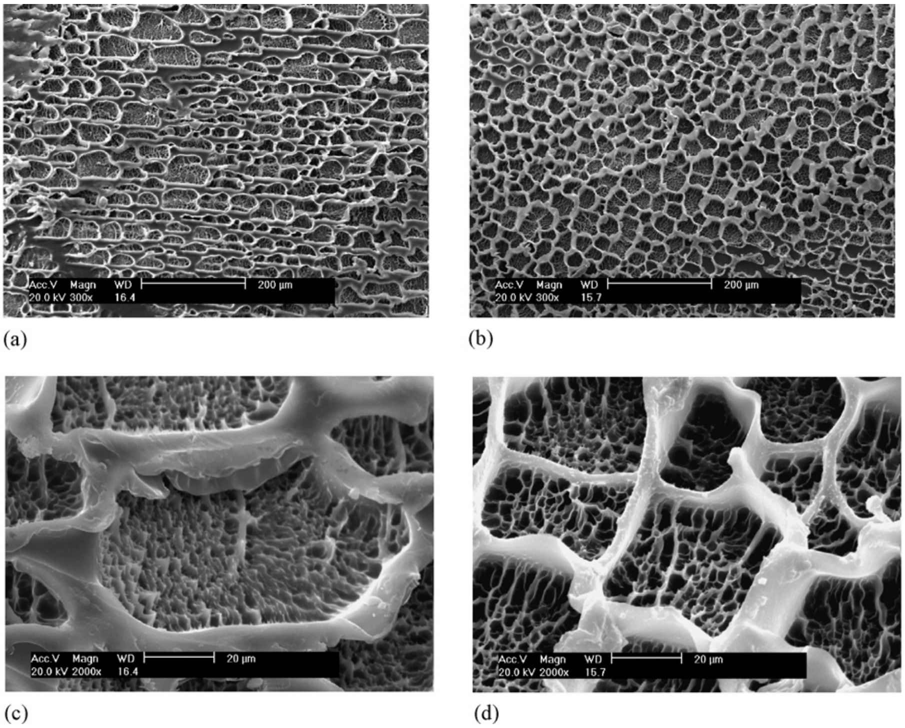

Fig. 2. (a) SEM micrographs of the swollen PN gel surface at 10 °C (magnification, 300×). (b) SEM micrographs of the swollen PM gel surface at 10 °C (magnification, 2000×). (c) SEM micrographs of the swollen PN gel surface at 10 °C (magnification, 2000×). (d) SEM micrographs of the swollen PM gel surface at 10 °C (magnification, 2000×).

The data in Table 1 indicate that the specific surface areas S_{BET}, the pore volume V_{pore} and average pore size D_{p} of the PM hydrogel were larger than those of the PN hydrogel. The S_{BET} of the PN hydrogels was 1.1 m^2/g, while the S_{BET} of the PM hydrogel was up to 10.3 cm^2/g. The V_{pore} of the PN hydrogel was $1.5 \times 10^{-3}\ \mathrm{m}^3/\mathrm{g}$, whereas the V_{pore} of the PN hydrogel was up to $2.7 \times 10^{-2}\ \mathrm{cm}^3/\mathrm{g}$. Also, the D_{p} of the PN hydrogel was 2.3 nm, which was somewhat smaller than that of the PM hydrogel (2.9 nm). It suggests that microwave irradiation could develop the porous structure of PNIPAAm hydrogel better.

3.3. *Swelling kinetics of PNIPAAm hydrogels*

In order to value or compare the response behavior of the PNIPAAm hydrogels, it is necessary to determine their swelling rates. Suppose M gram of dried hydrogel is suddenly submersed in distilled water below LCST. At time $t > 0$, swelling of the gel occurs, and q_t amount of water taken by the hydrogel increases with time. The swelling rate, r_{s}, is assumed to follow first-order kinetics with the following equation used to describe this swelling process [11]:

$$r_{\mathrm{s}} = -\frac{\mathrm{d}q_t}{\mathrm{d}t} = K_{\mathrm{s}}(q_{\mathrm{ms}} - q_t) \tag{1}$$

where K_{s} is the rate constant of the pseudo-first-order swelling model, q_{ms} is the swelling equilibrium amount of water uptake corresponding to some temperature, and q_t is the water amount taken by PNIPAAm hydrogel at time t from the aqueous solution, which can be found out using gravimetrical measurement method [6]. From Eq. (1), integral equation is available as follows:

$$\ln\left(\frac{1 - q_t}{q_{\mathrm{ms}}}\right) = -K_{\mathrm{s}}t \tag{2}$$

If swelling kinetic experiment of PNIPAAm hydrogel is conducted at the temperature below LCST, corresponding kinetic curve, q_t–t curve, could be obtained. After that, a plot of $-\ln(1 - q_t/q_{\mathrm{ms}})$ versus t will yield a line with slope K_{s}. As a result, from the slope of the line, K_{s} can be found out [12].

Figs. 3 and 4 show the swelling kinetic curves of the PN and PM gels. It can be seen that the water taken by the gels increased quickly during their initial swelling, then increased slowly and

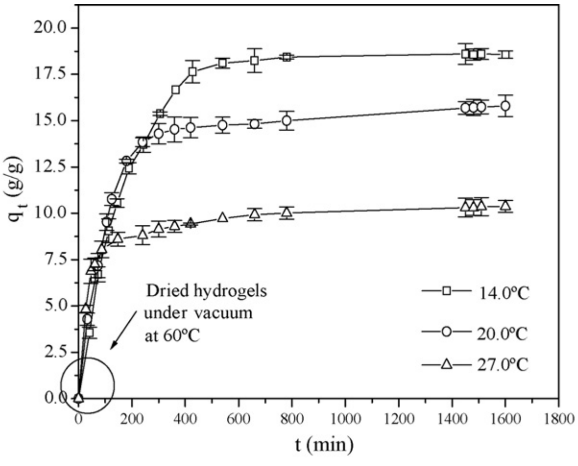

Fig. 3. PM swelling kinetic curves.

finally reached equilibrium amounts. The lower the temperature was, the larger the corresponding equilibrium amount of water taken by the gels.

During the swelling process, water needs continuously to overcome the osmotic pressure inside of the gel [13]. The lower the osmotic pressure, the faster the water permeates through the gel. According to the Flory–Rehner theory, there are three terms to describe this osmotic pressure in the general case of charged polymer networks [14]. They are mixing, elastic and ionic terms. In this work, non-polyelectrolyte gels existed and the swelling solution was pure water. Therefore, only the elastic pressure [15] was considered to control the swelling rate of the hydrogel. At the beginning of the swelling process, its osmotic pressure caused by low elasticity of the hydrogel was very low, and hence the hydrogel had a much higher swelling rate. As the process goes on, the elasticity of the hydrogel gradually increased with more water entering into the polymer network. As a result, water needed to overcome larger osmotic pressure and thus the swelling rate of the hydrogel would become smaller and smaller with the increase of the osmotic pressure.

It was noticed that the equilibrium amounts of water taken by the PM gel were larger than that of the PN gel at the same temperature. Generally speaking, a more porous matrix provides more space to accommodate water [6,16]. The PM gel had a more developed porous structure compared to the PN gel below LCST, as indicated in Table 1 and Fig. 2. As a result, the PM gel could accommodate much more water and thus had a higher equilibrium amounts q_m at the temperature below LCST. In addition, Figs. 3 and 4 also indicate that the times required for the water absorption of the hydrogels to reach equilibrium at different temperature were different. The equilibrium time was shortened with increasing water-bath temperature because diffusion of water molecular became quicker with temperature. Also, the equilibrium times for the PM gel were shorter than that for the PN gel at same temperature. It was mainly ascribable to the developed porous structure of the PM gel, as mentioned earlier. Its larger pore size made the diffusion of water molecular easier and faster during swelling process.

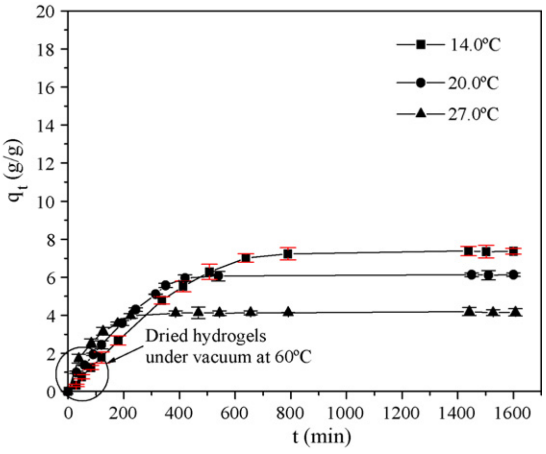

Fig. 4. PN swelling kinetic curves.

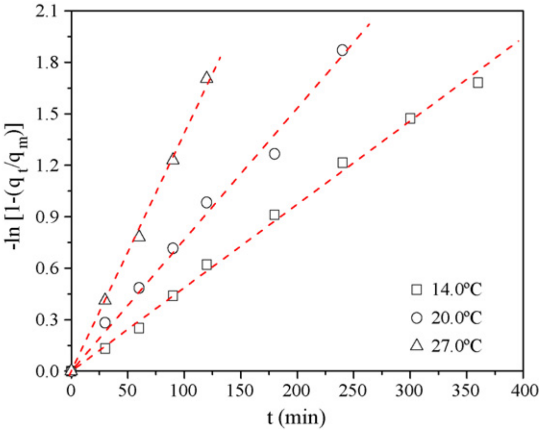

Fig. 5. Dependence of the $-\ln[1-(q_t/q_{ms})]$ of swelling PM gel on time.

Table 2
Swelling kinetic parameters of PNIPAAm hydrogels

	T^* (°C)		
	14.0	20.0	27.0
PM			
q_{ms}	20.38	17.11	13.37
K_s	5.32×10^{-3}	8.31×10^{-3}	15.11×10^{-3}
R^2	0.9983	0.9963	0.9991
PN			
q_{ms}	7.36	6.13	4.16
K_s	2.26×10^{-3}	3.59×10^{-3}	8.46×10^{-3}
R^2	0.9785	0.9785	0.9785

T^* is solution temperature (°C).

After swelling kinetic curves of the PN and PM gels were available, their swelling rate constants can be found out according to Eq. (2). Figs. 5 and 6 show the plots of $-\ln[1-(q_t/q_{ms})]$ versus time for swelling of the PM and PN gels. From the slopes of these lines, the swelling rate constants of the gels were obtained. Table 2 lists the swelling rate constants of the PM and PN gels as well as the correlation coefficients (R^2) for the linear regression of the data presented in Figs. 5 and 6. The linear correlation of the data was good because the correlation coefficients were up to 0.96.

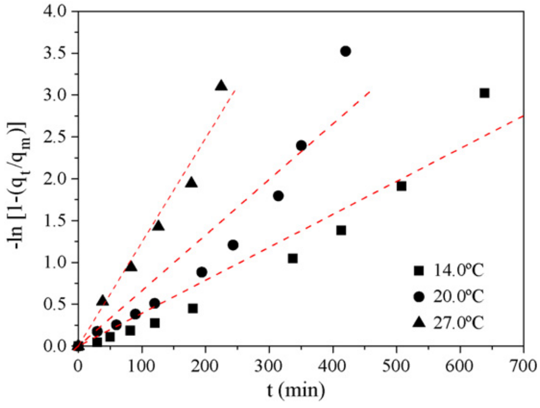

Fig. 6. Dependence of the $-\ln[1-(q_t/q_{ms})]$ of swelling PN gel on time.

The data in Table 2 indicate that the swelling rate of the PM hydrogel was about two times as fast as that of PN hydrogel. It was mainly ascribable to the PM gel having more developed porous structure, as shown in Fig. 1b, d and Table 1. The PM gel had not only larger area but also more pores in comparison with the PN gel. The more the pores of the gel were, the quicker the diffusion of water molecular from aqueous solution into pore surface was. It implies that the application of different preparation methods to synthesize hydrogels could result in differences of their porous structures, and thus make their swelling rate different. Some similar reports were obtained in Ref. [6]. Zhang et al. [6] also found that the hydrogels synthesized in mixed solvents had more porous and heterogeneous structures, which enabled the hydrogels to absorb large amounts of water and improved their temperature sensitivity. In this work, we found that the application of microwave irradiation to synthesize gels can produce more pores in the gel's network structure, which enabled PM gel to possess the larger swelling equilibrium ratio and faster swelling rate.

3.4. Deswelling kinetics of PNIPAAm hydrogels

In order to value or compare the response behavior of the PNIPAAm hydrogels, it is necessary to determine their deswelling rates. Suppose *M* gram of swollen hydrogel is suddenly submersed in distilled water above its LCST when the hydrogels were fully swollen at 14 °C. When time $t = 0$, $q_t = q_0$. At time $t > 0$, deswelling of the gel occurs, and q_t amount of water absorbed by the hydrogel decreases with time. The deswelling rate, r_d, is assumed to follow first-order kinetics with the following equation used to describe this deswelling process [8]:

$$r_\mathrm{d} = -\frac{\mathrm{d}q_t}{\mathrm{d}t} = K_\mathrm{d}(q_t - q_\mathrm{md}) \tag{3}$$

where K_d is the rate constant of the pseudo-first-order deswelling model, q_md is the deswelling equilibrium amount of water absorbed corresponding to some temperature, q_0 is the swelling equilibrium amount of water absorbed at 14 °C, and q_t is the water absorbed at time *t* from the aqueous solution, which can be found out using gravimetrical measurement method [6]. From Eq. (3), integral equation is available as follows:

$$\ln\left[\frac{q_t - q_\mathrm{md}}{q_0 - q_\mathrm{md}}\right] = -K_\mathrm{d}t \tag{4}$$

If deswelling kinetic experiment of PNIPAAm hydrogel is conducted at the temperature above LCST, corresponding deswelling kinetic curve, q_t–t curve, could be obtained. After that, a plot of $-\ln[(q_t - q_\mathrm{md})/(q_0 - q_\mathrm{md})]$ versus *t* will yield a line with slope $-K_\mathrm{d}$. As a result, from the slope of the line, K_d can be found out.

Figs. 7 and 8 represent the deswelling kinetic curves of the PN and PM gels. It can be seen that the amounts of water absorbed by the gels decreased quickly during initial deswelling, then decreased slowly and finally reached the equilibrium amounts. A comparison of these deswelling kinetic curves shows that the higher the temperature was, the faster the water release rate of the gels was. The deswelling rate increased with increasing water-bath temperature because diffusion of water molecular became quicker with the increase of temperature.

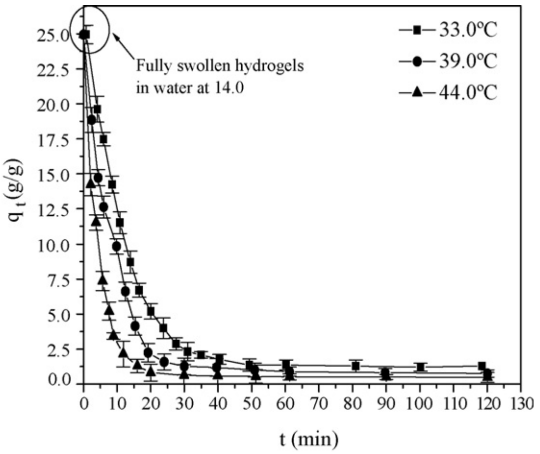

Fig. 7. PM deswelling kinetic curves.

According to deswelling kinetic curves of the PN and PM gels, their deswelling rate constants can be found out according to Eq. (4). Figs. 9 and 10 show that the plots of $-\ln[(q_t - q_\mathrm{md})/(q_0 - q_\mathrm{md})]$ versus time for deswelling of the PN and PM gels approached linear relation. From the slopes of these

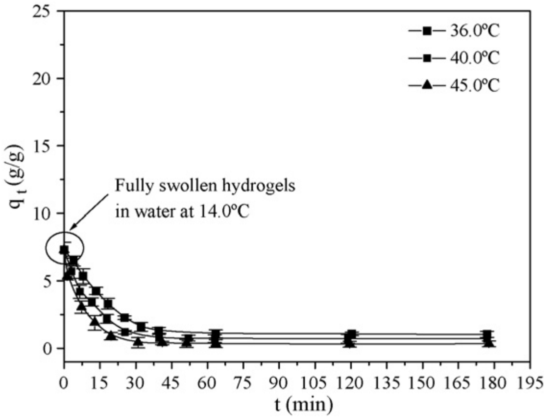

Fig. 8. PN deswelling kinetic curves.

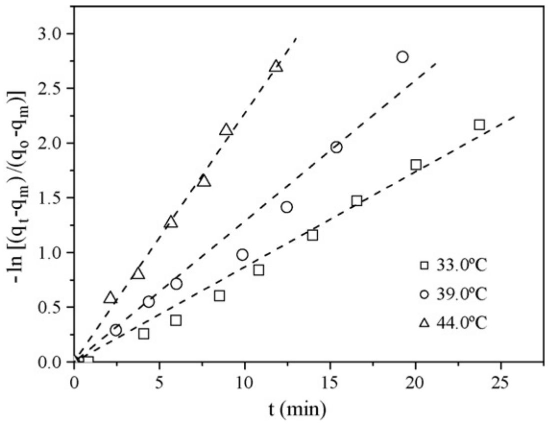

Fig. 9. Dependence of the $-\ln[(q_t - q_\mathrm{md})/(q_0 - q_\mathrm{md})]$ of deswelling PM gel on time.

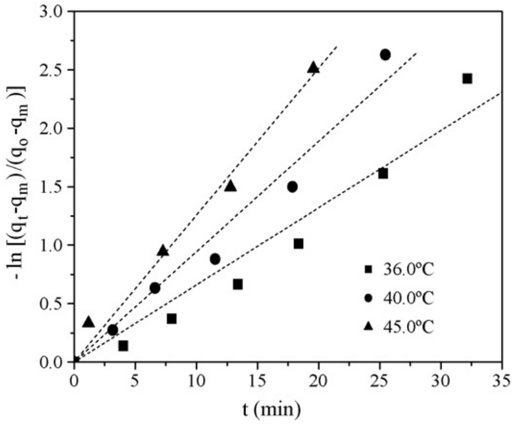

Fig. 10. Dependence of the $-\ln[(q_t - q_{\rm md})/(q_0 - q_{\rm md})]$ of deswelling PN gel on time.

lines, the deswelling rate constants of the gels were obtained, as listed in Table 3. The plots were linearly fitted with correlation coefficients of more than 0.96, indicating that the deswelling process can be apparently governed by the first-ordered manner. The data in Table 3 indicate that the deswelling rate constants of the PM gel were much larger than those of the PN gel. It implies that the preparation methods had influence on the responsive kinetics of the synthesized PNIPAAm hydrogels. Eder et al. [7] also found that the use of different preparation methods to synthesize PNIPAAm hydrogels had influence on their responsive kinetics. They used e-beam irradiation to synthesize PNIPAAm gel and then employed microscopy to observe the surface morphology of the synthesized hydrogels. It was observed that gels prepared by e-beam irradiation showed much higher porosity compared to the chemically crosslinked gels. Kinetic experiments showed that this resultant gel exhibited a four times higher swelling degree and a twenty times faster shrinking velocity in comparison with the gel synthesized by chemical crosslinking. In this work, we used microwave irradiation to synthesize the PNIPAAm hydrogel, and also found that resultant PM hydrogel had more porous structure, as shown clearly in SEM images (Fig. 2), in comparison with the PN gel prepared by hydrothermal method. As a result, the PM gel had faster responsive rate of swelling and desewlling compared to the PN gel.

3.5. *Determination of the activation energy for PNIPAAm hydrogels' swelling and deswelling*

According to the Arrhenius equation, suppose that the relationship between the rate constant K and the activation energy for PNIPAAm hydrogels' swelling and deswelling, E, can be described as follows:

Table 3
Deswelling rate constants of PN and PM hydrogels

	PM			PN		
	$T^{*a} = 33$	$T^{*a} = 39$	$T^{*a} = 44$	$T^{*a} = 36$	$T^{*a} = 40$	$T^{*a} = 45$
$q_{\rm md}/q_0$	0.052	0.033	0.019	0.140	0.097	0.045
$K_{\rm d}$	0.0869	0.1288	0.2275	0.0660	0.0944	0.1257
R^2	0.9980	0.9839	0.9972	0.9847	0.9847	0.9847

[a] T^* was solution temperature (°C).

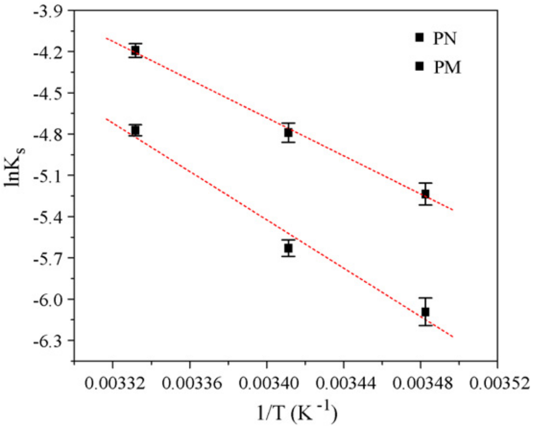

Fig. 11. Dependence of the $\ln K_{\rm s}$ on $1/T$ for swelling of PNIPAAm hydrogles.

$$K = A\exp\left(-\frac{E}{RT}\right) \tag{5}$$

where A is the rate coefficient and T is the solution temperature. Eq. (5) can also be expressed as

$$\ln K = \ln A - \left(\frac{E}{RT}\right) \tag{6}$$

When $\ln K$ is plotted to ($1/T$), a straight line (slope = $-(E/R)$) is obtained. The activation energy E can be directly calculated from the slope.

For swelling process, $K = K_{\rm s}$, $A = A_{\rm s}$, and $E = E_{\rm s}$. Eq. (6) can be expressed in its linear form as

$$\ln K_{\rm s} = \ln A_{\rm s} - \left(\frac{E_{\rm s}}{RT}\right) \tag{7}$$

For deswelling process, $K = K_{\rm d}$, $A = A_{\rm d}$, and $E = E_{\rm d}$. Eq. (6) can be expressed in its linear form as

$$\ln K_{\rm d} = \ln A_{\rm d} - \left(\frac{E_{\rm d}}{RT}\right) \tag{8}$$

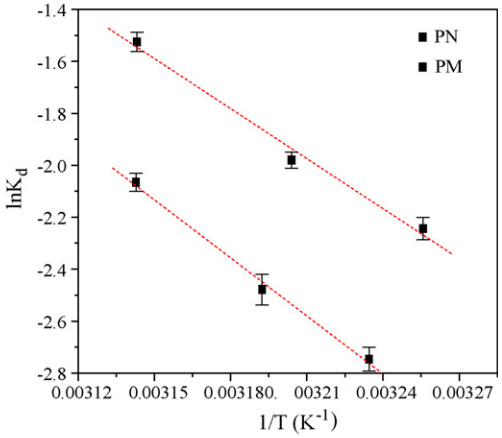

Fig. 12. Dependence of the $\ln K_{\rm s}$ on $1/T$ for deswelling of PNIPAAm hydrogles.

Table 4
Activation energy for swelling and deswelling of the PNIPAAm hydrogels

	Sample	
	PM	PN
E_s (kJ/mol)	57.84	75.08
A_s	1.73×10^8	4.21×10^{10}
E_d (kJ/mol)	53.48	58.74
A_d	1.27×10^8	7.95×10^8

Figs. 11 and 12 show the linear dependences between ln *K* and 1/*T* for swelling and deswelling of the PN and PM gels. Good linearity between ln *K* and 1/*T* was approximately in accordance with the Arrhenius equation. Their coefficients were more than 0.97.

Table 4 lists that swelling and deswelling activation energies of the PM and PN hydrogels. The data in Table 4 indicate that the swelling activation energies of the PNIPAAm hydrogels were higher than its deswelling activation energy, which suggesting that deswelling was much easier to execute compared to swelling. The basic reasons were as follows: according to Flory's mean-field theory [13,17], when the network of the hydrogels expanded the chemical potential difference between inside and outside the hydrogels would increase, which would lead to an increase in the osmotic pressure within the gel matrix. Once the temperature was increased above its LCST, the expanded hydrogel chains quickly dehydrated and exhibited rapid deswelling, resulting in the rapid deswelling kinetics. In addition, fast water diffusion within the expanded gel matrix with more and larger pores might also be a reason for the rapid deswelling kinetics.

Table 4 also indicates that deswelling activation energy of the PM gel was also somewhat lower than that of the PN gel. It illustrated that the deswelling behavior of the PM gel was easier than that of the PN gel due to the more and larger pores of the PM gels.

4. Conclusions

PNIPAAm hydrogels were synthesized separately by means of microwave irradiation and normal water-bath heating. Results of kinetic experiments showed that swelling and deswelling rates of the synthesized PNIPAAm hydrogels (PN and PM) increased with temperature, and the deswelling rates of these hydrogels were higher than their swelling rates. SEM analyses revealed that in comparison with the application of the water-bath heating method, the use of microwave irradiation method to prepare the hydrogel not only made it more porous, but also made its pores more uniform and deeper. Such a network structure of PM gels had their swelling/deswelling rate faster and its swelling/deswelling activation energy lower compared to PN gels.

Acknowledgements

The authors would like to thank the National Natural Science Foundation of China (No. 20606012) and the National Science Foundation of GuangDong Province (No.06300142) for financial support.

References

[1] X.Z. Zhang, C.C. Chu, Fabrication and characterization of microgel-impregnated, thermosensitive PNIPAAm hydrogels, Polymer 46 (2005) 9664–9673.
[2] Y. Hirokawa, T. Tanaka, Reentrant phase transition in acrylamide-derivation copolymer gels, J. Chem. Phys. 17 (1984) 2641–2643.
[3] H. Inomata, N. Wada, Y. Yagi, S. Goto, S. Saito, Swelling behaviours of *N*-alkylacrylamide gels in water: effects of copolymerization and crosslinking density, Polymer 36 (1995) 875–877.
[4] V.Y. Grinberg, A.S. Dubovik, D.V. Kuznetsov, N.V. Grinberg, A.Y. Grosberg, T. Tanaka, Studies of the thermal volume transition of poly(*N*-isopropylacrylamide) hydrogels by high-sensitivity differential scanning microcalorimetry. 2. Thermodynamic functions, Macromolecules 33 (2000) 8685–8692.
[5] G. Bokias, Y. Mylonas, Synthesis and aqueous solution properties of novel thermoresponsive graft copolymers based on a carboxymethylcellulose backbone, Macromolecules 34 (2001) 4958–4964.
[6] X.Z. Zhang, Y.Y. Yang, T.S. Chung, Effect of mixed solvents on characteristics of poly(*N*-isopropylacrylamide) gels, Langmuir 18 (2002) 2538–2542.
[7] L.M. Eder, L.C. Angel, C.B. Jose Manuel, K.F. Arndt, Effect of method of preparation on properties of temperature and pH-sensitive gels: chemical crosslinking versus irradiation with e-beam, React. Funct. Polym. 67 (2007) 67–80.
[8] T. Serizawa, K. Wakita, M. Akashi, Rapid deswelling of porous poly(*N*-isopropylacrylamide) hydrogels prepared by incorporation of silica particles, Macromolecules 35 (2002) 10–12.
[9] C.L. Bell, N.A. Peppas, Biomedical membranes from hydrogels and interpolymer complexes, Adv. Polym. Sci. 122 (1995) 125–175.
[10] S. Kuslu, M. Bayramoglu, Microwave-assisted dissolution of pyrite in acidic ferric sulfate solutions, Ind. Eng. Chem. Res. 41 (2002) 5145–5150.
[11] S. Meyer, W. Richtering, Influence of polymerization conditions on the structure of temperature-sensitive poly(*N*-isopropylacrylamide) microgels, Macromolecules 38 (2005) 1517–1519.
[12] K. Laszlo, K. Kosik, C. Rochas, E. Geissler, Phase transition in poly(*N*-isopropylacrylamide) hydrogels induced by phenols, Macromolecules 36 (2003) 7771–7776.
[13] J. Sun, J. Chen, L.M. Yang, S. Wang, Z.J. Li, H.F. Wu, Synthesis and characterization of a pH-sensitive hydrogel made of pyruvic-acid-modified chitosan, J. Biomater. Sci., Polym. Ed. 18 (1) (2007) 35–44.
[14] P.J. Flory, Principles of Polymer Chemistry, Principles of Polymer Chemistry, Cornell University Press, Ithaca, NY, 1953, pp. 24–250.
[15] I. Colombo, M. Grassi, M. Fermeglia, R. Lapasin, S. Pricl, Modeling phase transitions and sorption–desorption kinetics in thermo-sensitive gels for controlled drug delivery systems, Fluid Phase Equilibria 116 (1996) 148–161.
[16] H. Jian, X.L. Wang, W.S. Qi, X.H. Yu, Temperature sensitivity and electrokinetic behavior of a *N*-isopropylacrylamide grafted microporous polyethylene membrane, Desalination 146 (2002) 345–351.
[17] T. Tanaka, D.J. Fillmore, S.T. Sun, I. Nishio, G. Swislow, A. Shah, Phase transitions in ionic gels, Phys. Rev. Lett. 45 (1980) 1636–1639.